NSRRC-J04552(2014)

THE JOURNAL OF PHYSICAL CHEMISTRY B

Article

pubs.acs.org/JPCB

Effect of Molecular Properties of Random Copolymers on the Stability and Domain Dimension of Block Copolymer/Random Copolymer Blends

Chieh-Tsung Lo* and Po-Wei Chou

Department of Chemical Engineering, National Cheng Kung University, No. 1, University Road, Tainan City 701, Taiwan

Supporting Information

ABSTRACT: The morphological behavior of binary mixtures containing poly(styrene-*b*-2-vinylpyridine) (PS-*b*-PVP) diblock copolymer and poly(styrene-*r*-2-vinylpyridine) (PS-*r*-PVP) random copolymer was investigated as a function of the molecular weight ratio of PS-*b*-PVP and PS-*r*-PVP (R), the PS fraction in PS-*r*-PVP, and the concentration of PS-*r*-PVP in the blends (ϕ_r). When R was high, the addition of symmetric PS-*r*-PVP caused lateral expansion of microdomains and reduced the interdomain distance of the blend, indicating localization of PS-*r*-PVP at the PS-*b*-PVP interface. At high ϕ_r, packing constraints prevented all PS-*r*-PVP from assembling at the PS-*b*-PVP interface, which induced macrophase separation and formed a coexisting morphology composed of ordered polymer phase and random copolymer-rich regimes. Reducing the R value reduced the amount of PS-*r*-PVP that could be assembled at the PS-*b*-PVP interface, and macrophase separation occurred at a low PS-*r*-PVP content. When asymmetric PS-*r*-PVP was introduced into PS-*b*-PVP, PS-*r*-PVP was located in the preferred domain of PS-*b*-PVP because of the favorable interaction of PS-*r*-PVP with the particular domain. The enthalpically driven self-assembly rendered to swell the preferred domain and increased the interfacial curvature that, in turn, induced an order−order transition.

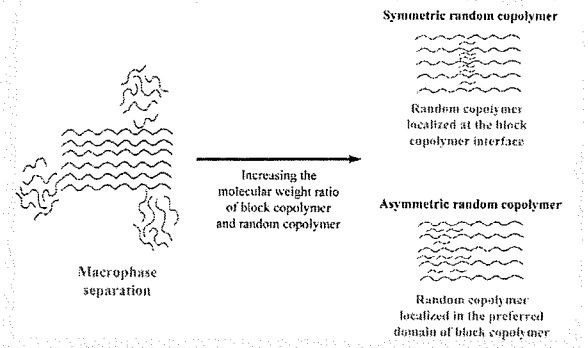

INTRODUCTION

Most polymer pairs are immiscible, and blends of two homopolymers tend to phase separate at macroscale-length scales. Unlike homopolymer mixtures, block copolymers, which constitute distinct types of polymer connected with covalent bonds, form microphase separation with domain dimensions of 10−100 nm. The microphase separation of block copolymers enables generating a wide range of periodic morphologies, such as lamellae, gyroids, hexagonally packed cylinders, and spheres.[1−3] Such self-assembly behavior renders block copolymers a candidate in a variety of nanotechnology applications, such as nanolithography, a reactor to synthesize nanoparticles, high-density arrays for use in data storage, photovoltaic devices, and gas separation.[4−8] Although block copolymers provide rich phase behavior and ordered phases, the most challenging aspect of the application of block copolymers is manipulating their morphology and the domain dimensions. Because the synthesis of block copolymers involves complex processes, the preparation of block copolymers with precise control of their molecular structures requires much efforts and high cost. An alterative approach to manipulating the molecular properties of block copolymers is polymer blending. Because of its ease of modifying the properties of polymers, polymer blends have many industrial applications.

Considerable effort has been exerted on exploring the phase behavior of block copolymer/homopolymer blends.[9−15] The addition of A homopolymer in the preferred domain of A−B block copolymer allows the homopolymer to increase the A-rich regions, which increases the domain size of the block copolymer. In addition, the expansion of the A domain in the block copolymer increases the interfacial curvature between A and B domains, leading to an order−order transition, forming new structures. The concept of controlling the morphology and domain dimensions of blends, such as the homopolymer molecular weight and concentration, is well understood. Another well-established blend system is the mixture of a block copolymer with another block copolymer with the same components but distinct chain lengths.[16−21] Unlike block copolymer/homopolymer blends in which homopolymers are confined in one domain of the block copolymer, in block copolymer blends, the junction points of the two block copolymers located at the same interfacial region and the same component in each block copolymer share the respective microphase-separated domains. This is called the cosurfactant effect. The miscibility limit and the phase transitions of the blends are highly sensitive to the long-range interactions involving the packing and distribution of chain lengths within the blend and the short-range segmental interactions.

Received: June 24, 2014
Revised: October 2, 2014
Published: October 20, 2014

 © 2014 American Chemical Society dx.doi.org/10.1021/jp5062607 | J. Phys. Chem. B 2014, 118, 12763−12771

In addition to the aforementioned studies, an extended study has been conducted on the mixture of a block copolymer and a random copolymer. Kressler et al. investigated the miscibility in blends consisting of polystyrene-*block*-poly(methyl methacrylate) block copolymer and poly(styrene-*random*-acrylonitrile) random copolymer.[22] A more extended region of miscibility in the blends was obtained when compared with the blends of polystyrene-*random*-poly(methyl methacrylate) and poly(styrene-*random*-acrylonitrile) random copolymers. Both theoretical predictions and experimental results suggested that the addition of a random copolymer in a block copolymer with the same monomer units could effectively lower the order−disorder transition temperature (T_{ODT}).[23,24] The suppression of T_{ODT} was pronounced when a low-molecular-weight random copolymer was added. Additionally, a phase diagram showed three regions: a homogeneous liquid phase region, an ordered mesophase region, and a two-phase region. Above T_{ODT}, the reduced interaction between the two components in the block copolymer facilitated homogeneous mixing with the random copolymer because of greatly increased mixing entropy with the addition of the random copolymer. By contrast, below T_{ODT}, the repulsive interaction between the two segments in the block copolymer was substantial, which induced microphase separation of the block copolymer, forming an ordered structure. Furthermore, when the fraction of random copolymer in the blend was greater than 0.15, macrophase separation was triggered.[25] The phase behavior of the blends could be manipulated by the monomer composition in the random copolymer, the concentration of the added random copolymer, the molecular weight of the random copolymer, and the annealing temperature. Kim et al.[26] further investigated the effect of the random copolymer composition on the phase behavior of block copolymer/random copolymer blends. They observed that the random copolymer with symmetric composition reduced T_{ODT} more effectively than the random copolymer with asymmetric composition did. Additionally, the random copolymer with symmetric composition preferred to localize at the interfacial area of the block copolymer to reduce the unfavorable contact of two segments at the interface, whereas the random copolymer with asymmetric composition tended to be confined in the preferred domain of the block copolymer.

In this study, we investigated the effect of added random copolymers on the phase behavior and domain dimension of a block copolymer. Our system interest is blends composed of a poly(styrene-*b*-2-vinylpyridine) (PS-*b*-PVP) diblock copolymer and poly(styrene-*r*-2-vinylpyridine) (PS-*r*-PVP) random copolymers. Although several studies have addressed the phase behavior of block copolymer/random copolymer blends, the fundamental understanding of these blends is incomplete compared with block copolymer/homopolymer and block copolymer/block copolymer blends. We modulated the phase behavior of the blends by changing the ratio of the molecular weight of the block copolymer to that of the random copolymer and the fraction of monomers in the random copolymers. The morphology and the domain dimensions of the blends were determined using transmission electron microscopy (TEM) and small-angle X-ray scattering (SAXS). Our results clearly illustrated the importance of the molecular weight ratio and the fraction of monomers in the random copolymers to tailoring the morphology of the blends. The self-assembled behavior resulted from the interplay between the preferential interaction between the block copolymer and the random copolymer and the entropic effects within the copolymers. No study has provided experimental data on the phase behavior of block copolymer/random copolymer blends as a function of the molecular weight ratio. Our results are quite complementary to the literature and can complete a story on the phase behavior of the block copolymer/random copolymer blends.

EXPERIMENTAL SECTION

Materials. Styrene, 2-vinylpyridine, calcium hydride (CaH_2), 2,2,6,6-tetramethylpiperidinooxy (TEMPO), and hexane were purchased from Sigma-Aldrich Co. Both styrene and 2-vinylpyridine were stirred with CaH_2 overnight and distilled under a vacuum prior to use. Azobisisobutyronitrile (AIBN) was provided by UniRegion Bio-Tech and used without further purification. Tetrahydrofuran (THF) was obtained from J. T. Baker. The poly(styrene-*b*-2-vinylpyridine) (PS-*b*-PVP) diblock copolymer and poly(styrene-*r*-2-vinylpyridine) (PS-*r*-PVP) random copolymers were purchased from Polymer Source unless otherwise stated.

Synthesis of PS-*r*-PVP Random Copolymers. PS-*r*-PVP random copolymers were synthesized through free radical bulk polymerization, using AIBN as the initiator.[27] Initially, styrene, 2-vinylpyridine, and TEMPO were introduced into a dry three-necked round-bottom flask with a stir bar under a nitrogen atmosphere. AIBN was added to the flask, and the mixture was heated in an oil bath at 85 °C for 3 h and at 125 °C for various reaction times. Because the reactivity ratios of styrene and 2-vinylpyridine are 0.50 and 1.27, respectively,[28] they have different tendencies to undergo copolymerization, leading to a composition drift. To prevent any composition drift for the synthesized random copolymers, the polymerization reaction was terminated at less than 20% of the conversion by cooling the reaction to room temperature.[27,29] The reaction mixture was then diluted with THF. The resultant polymer was purified through precipitation in hexane several times, and then dried in a vacuum oven.

The number-averaged molecular weight and polydispersity of the copolymers were characterized using gel permeation chromatography (GPC, Schambeck RI2000). GPC measurements were conducted using THF as the elution solvent at an elution rate of 0.5 mL/min. The instrument was calibrated with a polystyrene standard. The ^1H NMR spectra were recorded in $CDCl_3$ on a Bruker AV-500 Spectrometer to determine the fraction of PS and PVP in the copolymer. Fourier transform infrared spectroscopy (FTIR) was preformed on a Scinco/Nicolet 5700 spectrometer at a resolution of 2 cm^{-1}.

Preparation of Blends. The blends of PS-*b*-PVP and PS-*r*-PVP were prepared by dissolving both copolymers in THF. Table 1 provides the molecular properties of these copolymers. These mixtures were stored under ambient conditions for at least 3 days. The polymer solutions were then cast on both epoxy resin and Kapton to prepare bulk specimens. After 1 day of drying under a vacuum, the samples were annealed at 170 °C for 7 days.

Small Angle X-ray Scattering (SAXS). SAXS measurements were performed both at Sector 23A1 at the National Synchrotron Radiation Research Center in Taiwan and using a Bruker diffractometer (NanoSTAR U System, Bruker AXS Gmbh, Karlsruhe, Germany) to characterize the nanostructure of the blends. Samples on Kapton were measured at room temperature with a sample-to-detector distance of 2 m. The data were corrected for incident flux, absorption, detector sensitivity variation, and dark current.

Transmission Electron Microscopy (TEM). The blends embedded in epoxy resins were microtomed to a thickness of

dx.doi.org/10.1021/jp5062607 | J. Phys. Chem. B 2014, 118, 12763−12771

Table 1. Characteristics of Polymers

polymer	M_n (g/mol)	polydispersity index (PDI)	styrene fraction (f_{PS})	materials
PS-*b*-P2VP	80500	1.10	0.51	Polymer Source
PS-*r*-P2VP	1800	1.64	0.18	synthesis
	2300	1.58	0.48	synthesis
	2800	1.48	0.66	synthesis
	6300	1.75	0.50	synthesis
	10400	1.70	0.50	synthesis
	24500	1.50	0.46	Polymer Source
	28000	1.38	0.78	Polymer Source
	28500	1.57	0.23	Polymer Source
	58000	1.70	0.45	Polymer Source
	71000	1.60	0.44	Polymer Source

approximately 80 nm with an Ultracut R microtome (Reichert, Leica, MI, USA). To distinguish between the PS and PVP phases, the specimens were selectively stained with iodine vapor for 24 h. Iodine adsorbs to PVP that reveals as dark regions in TEM. A Hitachi H7500 transmission electron microscope operated at 100 kV was used to analyze the morphology of the blends.

RESULTS AND DISCUSSION

Phase Behavior of Block Copolymer/Random Copolymer Blends as a Function of the Molecular Weight of a Random Copolymer. We varied the molecular weight of PS-*r*-PVP, whereas the PS fraction in PS-*r*-PVP was fixed at approximately 0.5. To quantify the phase behavior of the copolymer blends regarding the molecular weight of PS-*r*-PVP, we defined the ratio of the molecular weight of PS-*b*-PVP to that of PS-*r*-PVP as *R*. Figure 1a shows the SAXS profiles of PS-*b*-PVP/PS-*r*-PVP (M_n = 2300 g/mol) blends where $R \approx 35$. As evidenced by the SAXS profiles, the neat PS-*b*-PVP exhibited diffraction peaks at a peak position ratio of 1:2:3:4:5:6, suggesting the formation of highly ordered lamellae. With the addition of PS-*r*-PVP, the higher order peaks gradually disappeared. However, multiple reflections with an integer ratio still existed, indicating that the morphology of the blends remained unchanged and the addition of PS-*r*-PVP did not disturb the ordered phases of the blends. Another feature in the SAXS patterns is the shift of the first order peak position to the higher *q* (scattering vector) with an increase in the PS-*r*-PVP content. According to the Bragg law, the interdomain distance (D) is correlated to the position of the first order peak (q^*) by $D = 2\pi/q^*$ for the lamellar phases. By this expression, the calculated interdomain distance decreased from 56.10 nm for the neat PS-*b*-PVP to 53.25, 49.87, 46.89, and 46.89 nm with the addition of 10, 20, 30, and 40% PS-*r*-PVP, respectively. The reduction of the interdomain distance with the addition of PS-*r*-PVP might be attributable to the localization of PS-*r*-PVP at the interface of PS-*b*-PVP microdomains.[26] As indicated by Gersappe and Balazs,[30] a random copolymer tends to accumulate at the interface of two immiscible polymers to screen the unfavorable monomer contacts at the interfaces. Thus, the random copolymer serves as a compatibilizer to reduce the interfacial tension in which the symmetric random copolymer is more effective in promoting the interfacial adhesion. By locating the random copolymer at the interface, the reduced interaction between PS and PVP molecules, defined as an effective χ parameter (χ_{eff}), can be calculated using the following expression:[31,32]

$$\chi_{eff} = \chi(f_{A1} - f_{A2})^2 \quad (1)$$

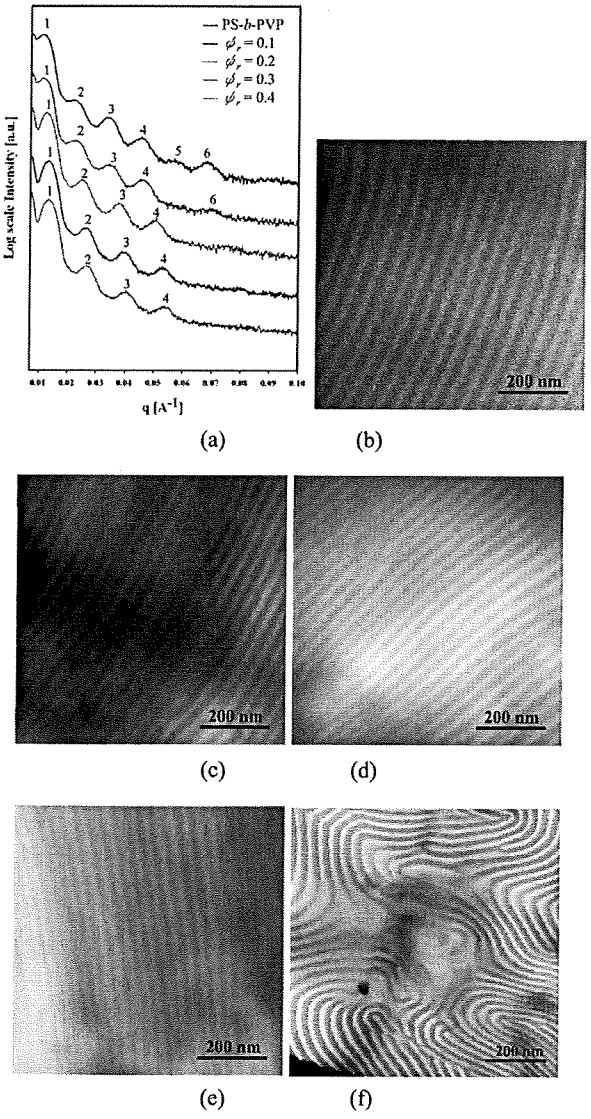

Figure 1. (a) SAXS of PS-*b*-PVP (M_n = 40500-*b*-40000 g/mol)/PS-*r*-PVP (M_n = 2300 g/mol, styrene fraction = 0.48) blends. TEM micrographs of (b) neat PS-*b*-PVP, (c) ϕ_r = 0.1, (d) ϕ_r = 0.2, (e) ϕ_r = 0.3, and (f) ϕ_r = 0.4. Scattering patterns have been shifted to increase clarity, and the numbers in the plot show the ratio of the peak positions to the value of the first-order peak.

where χ is the interaction parameter between PS and PVP segments, and f_{A1} and f_{A2} are the volume fraction of a given component in copolymer *i*. The calculated χ_{eff} was 0.0016χ for PS-*r*-PVP localized at the interface between PS and PVP microdomains.

When PS-r-PVP intervenes in the interface between PS-*b*-PVP microdomains, the change in the average nearest-neighbor distance of chemical junction points along the interface of the lamellar microdomains (a_J/a_{Jo}) can be estimated by

$$\frac{a_J}{a_{Jo}} = \left(\frac{\rho_{Jo}}{\rho_J}\right)^{1/2} = \left[\left(\frac{D_o}{D}\right)\phi_b^{-1}\right]^{1/2} \quad (2)$$

where a_{Jo} and a_J are the average nearest-neighbor distances between the chemical junctions along the interface without and

dx.doi.org/10.1021/jp5062607 | J. Phys. Chem. B 2014, 118, 12763−12771

with the addition of a random copolymer, ρ_{J_0} and ρ_J are the number of block chains per unit of interfacial area for the neat block copolymer and its blend with a random copolymer, D/D_o is the average interdomain distance of a blend relative to that of the neat block copolymer, and ϕ_b is the volume fraction of the block copolymer. With the addition of the random copolymer, ρ_J/ρ_{J_0} reduced to 0.84, 0.71, 0.58, and 0.48, which corresponded to the increase in a_J/a_{J_0} to 1.09, 1.19, 1.31, and 1.45 for 10, 20, 30, and 40% PS-*r*-PVP, respectively. These results indicated that the sequestering of PS-*r*-PVP at the interface expanded the chemical junction of PS and PVP blocks, causing the lateral expansion of microdomains parallel to the interface. This in turn compressed the two domains normal to the interface. Regarding the block copolymer/homopolymer blends in which a homopolymer dispersed uniformly in the preferred domain of the block copolymer,[9,10,12,13] the inclusion of a homopolymer swelled the preferred domain, which increased both the interdomain distance and the interfacial curvature. Consequently, an order–order transition occurred. By contrast, the distribution of a random copolymer at the interface did not alter the interfacial curvature. Therefore, an order–order transition did not occur. Similar behavior was observed when a graft copolymer was incorporated into the interface of a block copolymer.[33]

Complementarily, we used TEM to determine the structural features of these blends. The neat PS-*b*-PVP in Figure 1b clearly indicates the formation of a lamellar structure. The addition of low-concentration PS-*r*-PVP did not affect the development of lamellae. At ϕ_r = 0.4 where ϕ_r was the volume fraction of PS-*r*-PVP in the blend, however, a coexisting morphology composed of lamellae and a disordered structure was observed, indicating the macrophase separation of the random copolymer from the microdomains of the block copolymer. As indicated by the SAXS results, PS-*r*-PVP was located at the interface of PS-*b*-PVP. As the PS-*r*-PVP content increased, the available volume in the interface became saturated, and the excess PS-*r*-PVP could not be incorporated into the PS-*b*-PVP interface. Consequently, PS-*r*-PVP was expelled from the ordered phase of PS-*b*-PVP, forming the random copolymer-rich regimes. This morphological transition upon the addition of PS-*r*-PVP is consistent with the change in the interdomain distance. The interdomain distance of the blends reached a plateau when ϕ_r = 0.3, suggesting that the solubility limit for the blends without causing macrophase separation was when less than 30% PS-*r*-PVP was added.

Figure 2 shows the phase behavior of PS-*b*-PVP blended with PS-*r*-PVP with a molecular weight of 6300 g/mol ($R \sim 13$). The SAXS in Figure 2a clearly shows the formation of a lamellar structure regardless of the blend composition. The interdomain distance calculated from the position of the first order reflection decreased from 56.10 nm for the neat PS-*b*-PVP to 51.93 nm with the addition of 10% PS-*r*-PVP. The interdomain distance was constant with further incorporation of PS-*r*-PVP, indicating that only 10% PS-*r*-PVP could be localized at the interface of PS-*b*-PVP. The TEM micrographs in Figure 2b and c agree with the SAXS results. The blend containing 10% PS-*r*-PVP exhibited a lamellar structure. The addition of a greater amount of PS-*r*-PVP caused macrophase separation, forming a coexistence of polymer ordered phases and random copolymer-rich phases.

On the basis of the results of the self-assembly of the PS-*b*-PVP/PS-*r*-PVP blends, we categorized the resulting structure into two classes, including lamellae and macrophase separation. The phase behavior of these blends is summarized in Figure 3 according to these definitions. It was determined that the transition from lamellae to a coexisting structure depends heavily

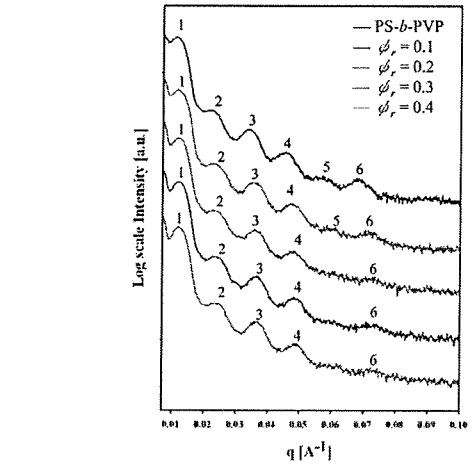

(a)

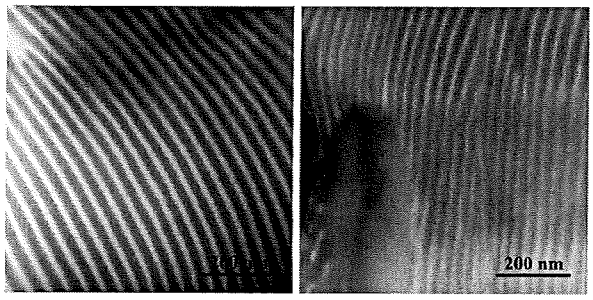

(b) (c)

Figure 2. (a) SAXS of PS-*b*-PVP (M_n = 40500-*b*-40000 g/mol)/PS-*r*-PVP (M_n = 6300 g/mol, styrene fraction = 0.5) blends. TEM micrographs of (b) ϕ_r = 0.1 and (c) ϕ_r = 0.4. Scattering patterns have been shifted to increase clarity, and the numbers in the plot show the ratio of the peak positions to the value of the first-order peak.

on the molecular weight ratio. When the molecular weight of PS-*b*-PVP was much larger than that of PS-*r*-PVP, the transition occurred at ϕ_r = 0.4. In this case, the molecular weight of PS-*r*-PVP was relatively small, and PS-*r*-PVP was able to locate at the interface between the PS and PVP domains of PS-*b*-PVP. By contrast, the positioning of a high-molecular-weight PS-*r*-PVP at the interfacial area of PS-*b*-PVP caused the substantial chain stretching of PS-*b*-PVP, which reduced the conformational entropy. To recover the entropy, PS-*r*-PVP was segregated from the ordered phases of PS-*b*-PVP, inducing macrophase separation. Although the formation of random copolymer-rich phases reduced the translational entropy, the increase in the conformational entropy outweighed the loss of the translational entropy. Consequently, the phase transition occurred at a low PS-*r*-PVP content when the molecular weight of PS-*r*-PVP was high.

Phase Behavior of Block Copolymer/Random Copolymer Blends as a Function of the Composition of a Random Copolymer. In this section, the ratio of the molecular weight of the block copolymer to that of a random copolymer was maintained at approximately 3, and the phase behavior of the PS-*b*-PVP/PS-*r*-PVP blends was investigated by changing the PS fraction in PS-*r*-PVP. Figure 4a shows the SAXS profiles of the PS-*b*-PVP/PS-*r*-PVP blends with a PS fraction in PS-*r*-PVP of 0.78. All the blends exhibited a lamellar structure. However, the interdomain distance of all the blends was invariant, implying

dx.doi.org/10.1021/jp5062607 | J. Phys. Chem. B 2014, 118, 12763–12771

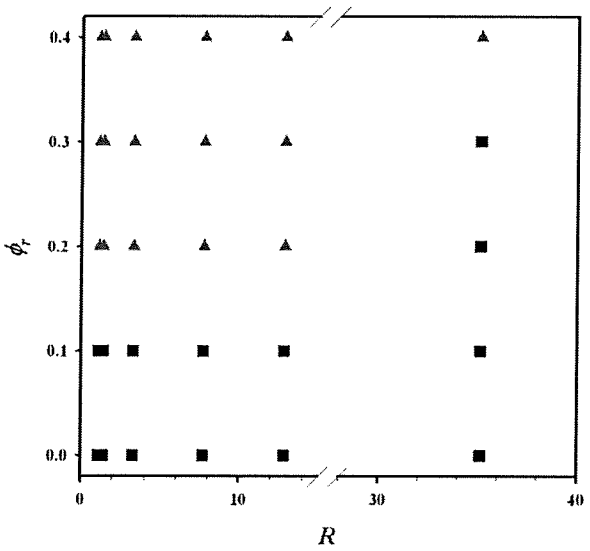

Figure 3. Phase behavior of PS-*b*-PVP/PS-*r*-PVP blends as a function of the molecular weight ratio and the random copolymer content. The PS fraction in PS-*r*-PVP is approximately 0.5. (■) Lamellae; (▲) macrophase separation.

that PS-*r*-PVP did not correlate to the ordered phases of PS-*b*-PVP. The TEM images in Figure 4b–f confirmed the behavior. Macrophase separation occurred, which was indicated by the lamellae for PS-*b*-PVP and the featureless region for PS-*r*-PVP. The disordered region increased with the addition of PS-*r*-PVP, but the lamellae were still observed at ϕ_r = 0.4. Kim et al.[26] suggested that, when an asymmetric random copolymer is incorporated into a block copolymer, the random copolymer acts as a homopolymer that is sequestered into the preferred domain of the block copolymer. This simultaneously increases the domain size. In our study, the PS fraction in PS-*r*-PVP was 0.78, but we did not observe the partition of PS-*r*-PVP in the PS domain of PS-*b*-PVP. Instead, the blends formed macrophase separation, which was presumably caused by the high-molecular-weight PS-*r*-PVP. The dispersion of the high-molecular-weight PS-*r*-PVP in the preferred domain of PS-*b*-PVP provided additional entropic loss. Hence, PS-*r*-PVP failed to solubilize in either domain of PS-*b*-PVP, and complete segregation occurred. Similarly, in the mixtures of a homopolymer and a block copolymer, Tanaka et al. suggested that, when the molecular weight of the homopolymer is comparable to that of a block copolymer, the homopolymer is expelled completely from the microdomains of the block copolymer.[10] Both blend systems exhibited the same entropically driven self-assembled behavior, and the stability of the blends could be manipulated by the relative molecular weight of the polymers in the blends.

We further increased the R value to approximately 35 and investigated the effect of PS-*r*-PVP composition on the phase behavior of the PS-*b*-PVP/PS-*r*-PVP blends. Figure 5 represents the phase behavior of PS-*b*-PVP/PS-*r*-PVP blends with a PS fraction in PS-*r*-PVP of 0.18. In the SAXS profiles shown in Figure 5a, when the PS-*r*-PVP content was below 30%, the blends exhibited a lamellar structure. At ϕ_r = 0.4, two peaks appeared at the scattering vector ratio of $1:(7)^{1/2}$, indicating that the blend developed to the hexagonally packed cylinders. The cylindrical structure was also confirmed by the micrograph shown in Figure 5b. This result suggested that the addition of this random

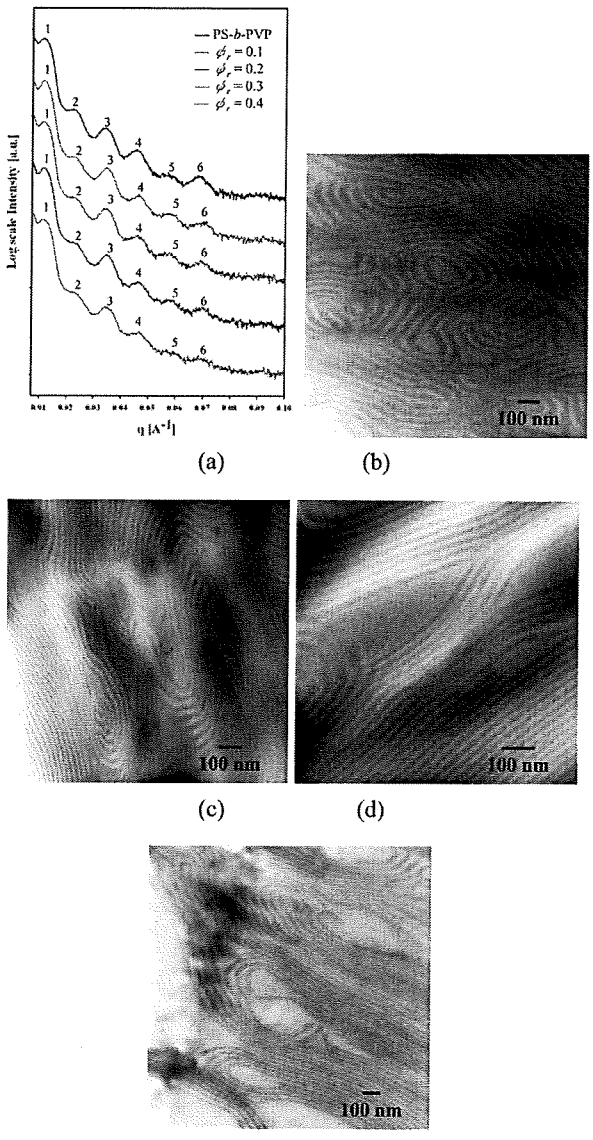

Figure 4. (a) SAXS of PS-*b*-PVP (M_n = 40500-*b*-40000 g/mol)/PS-*r*-PVP (M_n = 28000 g/mol, styrene fraction = 0.78) blends. TEM micrographs of (b) ϕ_r = 0.1, (c) ϕ_r = 0.2, (d) ϕ_r = 0.3, and (e) ϕ_r = 0.4. Scattering patterns have been shifted to increase clarity, and the numbers in the plot show the ratio of the peak positions to the value of the first-order peak.

copolymer induced an order–order transition. Furthermore, the calculated interdomain distance from SAXS increased from 56.10 nm for the neat PS-*b*-PVP to 57.64, 58.72, 59.47, and 63.20 nm for 10, 20, 30, and 40% PS-*r*-PVP, respectively. The increase of the interdomain distance suggested that the added PS-*r*-PVP was located in the preferred domain of PS-*b*-PVP. For this asymmetric PS-*r*-PVP, according to eq 1, the χ_{eff} values of the PS-*r*-PVP localized into the interface of PS-*b*-PVP, the PS microdomains, and the PVP microdomains are 0.1089χ, 0.06724χ, and 0.0324χ, respectively. Because the localization of PS-*r*-PVP into the PVP microdomains exhibited the minimum enthalpic cost, the asymmetric PS-*r*-PVP was able to be confined

dx.doi.org/10.1021/jp5062607 | J. Phys. Chem. B 2014, 118, 12763–12771

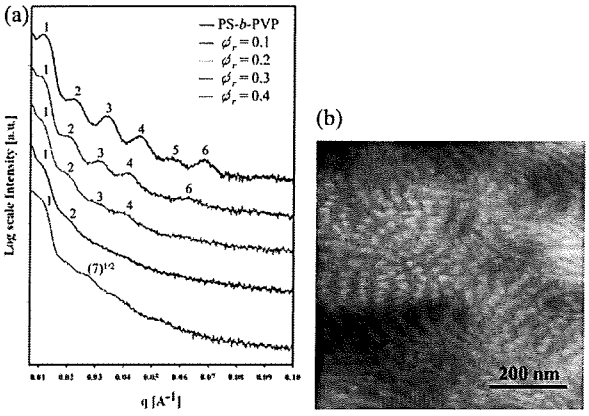

Figure 5. (a) SAXS of PS-*b*-PVP (M_n = 40500-*b*-40000 g/mol)/PS-*r*-PVP (M_n = 1800 g/mol, styrene fraction = 0.18) blends and (b) TEM micrographs of ϕ_r = 0.4. Scattering patterns have been shifted to increase clarity, and the numbers in the plot show the ratio of the peak positions to the value of the first-order peak.

in the PVP domains. In eq 1, the transition of the PS-*r*-PVP location occurred when the fraction of one component in PS-*r*-PVP was 0.25. When the PS fraction in PS-*r*-PVP was between 0.25 and 0.75, the localization of PS-*r*-PVP at the interface of PS-*b*-PVP had a lower enthalpy than that in either of the microdomains of PS-*b*-PVP. By contrast, when the PS fraction in PS-*r*-PVP was >0.75 or <0.25, the PS-*r*-PVP had higher solubility in the PS or PVP domains of PS-*b*-PVP. This thermodynamic aspect was also verified by Kim et al.[26] In their study, the location of poly(styrene-*random*-butadiene) (PS-*r*-PB) random copolymer moved from the interface to the PB domains of poly(styrene-*block*-butadiene) block copolymer when the PS fraction in PS-*r*-PB decreased from 0.5 to 0.25.

Figure 6 summarizes the phase diagrams of PS-*b*-PVP/PS-*r*-PVP blends as a function of the random copolymer composition and concentration. When $R \approx 3$ (Figure 6a), because the molecular weight of PS-*r*-PVP was comparable to that of PS-*b*-PVP, PS-*r*-PVP was unable to assemble in the microdomains of PS-*b*-PVP, and thus formed a coexisting structure. In this case, the incorporation of PS-*r*-PVP would cause chain stretching of PS and PVP chains in PS-*b*-PVP, which decreased the conformational entropy. By expelling PS-*r*-PVP from the microdomains of PS-*b*-PVP, the system gained the conformational entropy, although it lost the translational entropy. Therefore, the macrophase separation was entropically driven and it was independent of the monomer fraction in PS-*r*-PVP. Conversely, when $R \approx 35$ (Figure 6b), the incorporation of low-molecular-weight PS-*r*-PVP did not cause a considerable entropic penalty. The self-assembly of PS-*r*-PVP depended on the monomer fraction in PS-*r*-PVP. For symmetric PS-*r*-PVP, the localization of PS-*r*-PVP at the PS-*b*-PVP interface effectively reduced the interaction parameter between PS and PVP segments. By contrast, the asymmetric PS-*r*-PVP tended to distribute in the preferred domains of PS-*b*-PVP. The self-assembled behavior of PS-*r*-PVP in PS-*b*-PVP as a function of the monomer fraction in PS-*r*-PVP was enthalpically driven.

Change in Domain Dimensions in PS-*b*-PVP/PS-*r*-PVP Blends. Figure 7 shows the change in the domain dimensions of the PS-*b*-PVP/PS-*r*-PVP blends as a function of the molecular weight ratio and the PS fraction in PS-*r*-PVP. In the blends composed of a block copolymer and a polymer, if the polymer

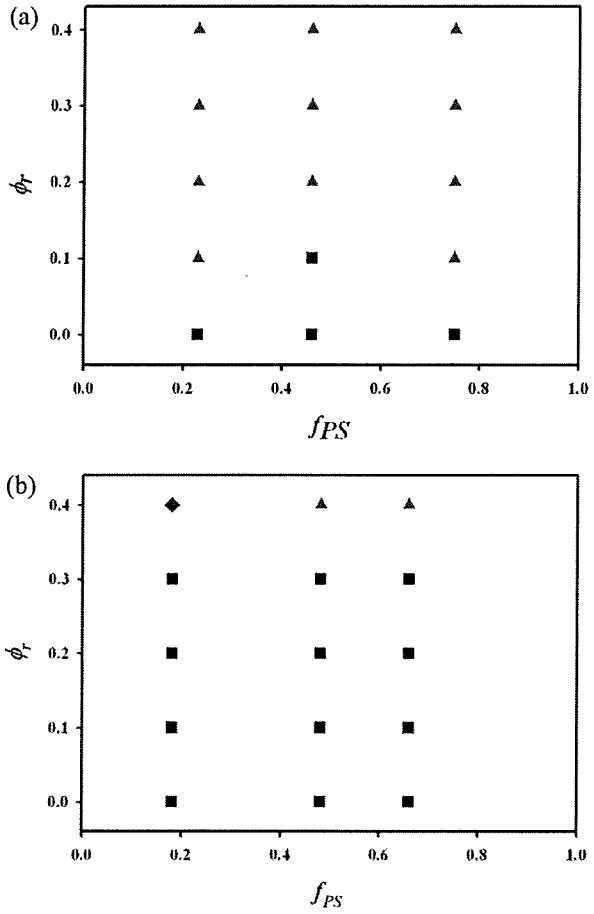

Figure 6. Phase behavior of PS-*b*-PVP/PS-*r*-PVP blends as a function of the random copolymer composition and concentration. (a) $R \approx 3$; (b) $R \approx 35$. (■) Lamellae; (▲) macrophase separation; (◆) hexagonally packed cylinders.

was localized at the center of the preferred domain of the block copolymer without disturbing the distances between the copolymer junctions, the microdomains only extended perpendicular to the interface. Thus, the change in the interdomain distance regarding the addition of the polymer is expressed by[34]

$$\frac{D}{D_o} = \frac{2 - \phi_p}{2(1 - \phi_p)} \tag{3}$$

where ϕ_p is the volume fraction of the polymer in the preferred domain of the block copolymer. By contrast, if the addition of the polymer causes the contraction of the microdomains as a result of the increase in the distances between copolymer junctions, the change in the interdomain distance can be expressed by[35]

$$\frac{D}{D_o} = (1 - \phi_p)^{2/3} \tag{4}$$

As shown in Figure 7, the most pronounced behavior of the change in the interdomain distance was that the interdomain distance of the blends reached a plateau with the addition of PS-*r*-PVP. The critical volume fraction to reach the plateau depended heavily on the values of R and f_{PS}. For instance, with the nearly identical f_{PS} (Figure 7a), the critical volume fraction

dx.doi.org/10.1021/jp5062607 | J. Phys. Chem. B 2014, 118, 12763−12771

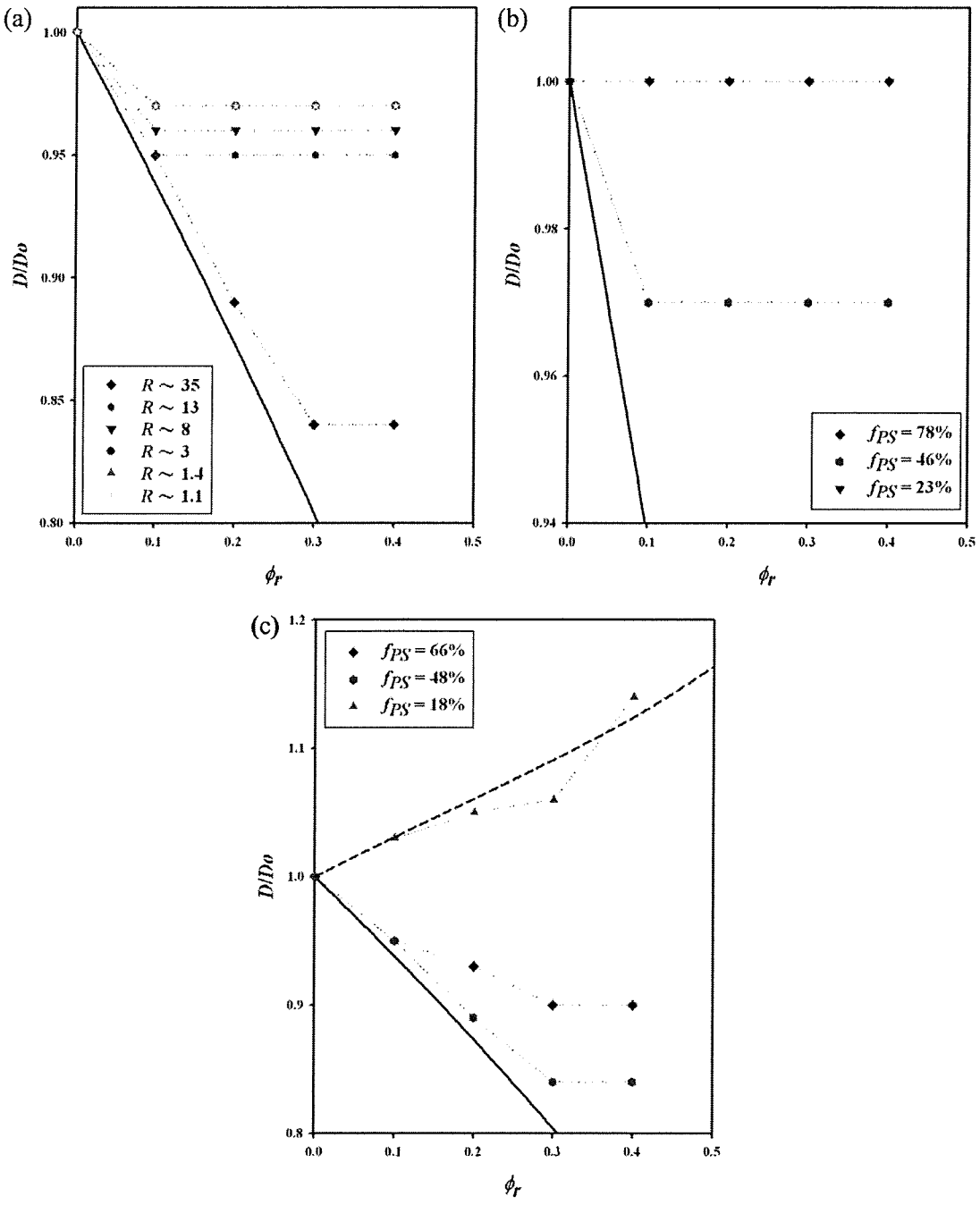

Figure 7. Interdomain distance of various PS-*b*-PVP/PS-*r*-PVP blends. As a function of (a) the molecular weight ratio ($f_{PS} \approx 0.5$) and the styrene fraction (b) $R \approx 3$ and (c) $R \approx 35$. The solid line is obtained from eq 4, whlie the dashed line is obtained from eq 3. The interdomain distance of the blends forming hexagonally packed cylinders was calculated by $(4/3)^{1/2} \times (2\pi/q^*)$.[9]

for $R \approx 35$ was 0.3, whereas that for $R \approx 1.4$ was 0.1. On the basis of a comparison of the value of the critical volume fraction of each blend with the aforementioned phase diagrams, the volume fraction of PS-*r*-PVP to induce a coexisting structure was identical to the critical volume fraction. When the macrophase separation of two copolymers occurred, the random copolymer could not be incorporated into the ordered domains of the block copolymer. Hence, the addition of the random copolymer did not affect the interdomain distance of the block copolymer, and hence the interdomain distance reached a constant value.

As shown in Figure 7a, when the symmetric PS-*r*-PVP was blended with PS-*b*-PVP, the interdomain distance decreased as the random copolymer fraction increased within the solubility limit. The change in the interdomain distance of the blends, particularly in the system of the small R value, closely matched the theoretical prediction determined using eq 4, suggesting that

dx.doi.org/10.1021/jp5062607 | J. Phys. Chem. B 2014, 118, 12763−12771

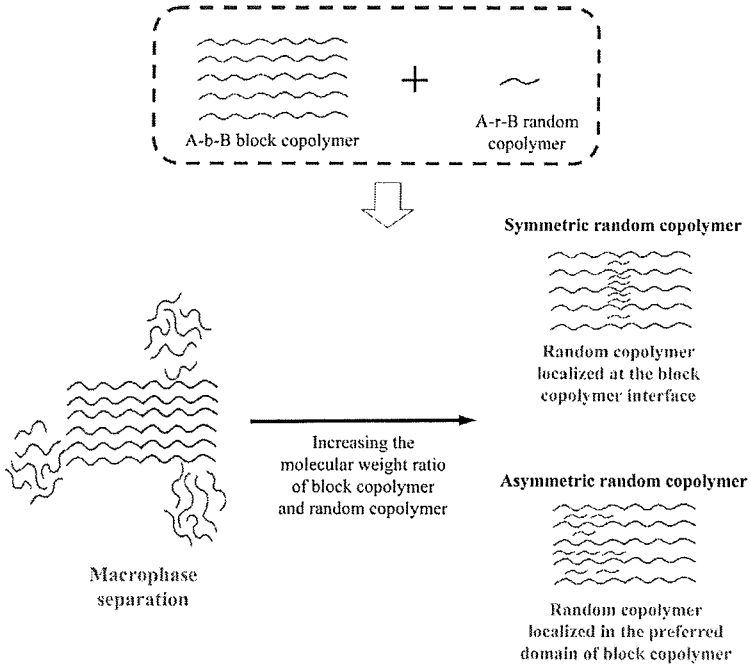

Figure 8. Schematic illustration of the phase behavior of block copolymer/random copolymer blends.

the introduction of low-molecular-weight PS-*r*-PVP effectively induces the lateral expansion of PS-*b*-PVP and decreases the interdomain distance. When $R \approx 35$ and f_{PS} was varied (Figure 7c), the introduction of PS-*r*-PVP could either increase or decrease the interdomain distance of PS-*b*-PVP, depending on the f_{PS} value. When f_{PS} was 0.18, the change in the interdomain distance was close to the prediction that PS-*r*-PVP was segregated to the center of the preferred domain of PS-*b*-PVP. Increasing the f_{PS} value as being a more symmetric PS-*r*-PVP led to a decrease in the interdomain distance with the addition of PS-*r*-PVP. The largest reduction of the interdomain distance was obtained when PS-*r*-PVP with f_{PS} of 0.5 was added to PS-*b*-PVP, indicating that the location of PS-*r*-PVP was gradually shifted from the preferred domain to the interface of PS-*b*-PVP. These results suggested that we can manipulate the ordered phases and domain dimensions of the block copolymer/random copolymer blends by simply changing the molecular parameters of the random copolymer.

■ CONCLUSION

The morphology and domain dimension of PS-*b*-PVP/PS-*r*-PVP blends were studied using SAXS and TEM. The phase behavior of these blends shows a strong dependence on the molecular weight ratio of PS-*b*-PVP and PS-*r*-PVP, the composition of PS-*r*-PVP, and the concentration of PS-*r*-PVP in the blends. The solubility model and the corresponding change in the domain dimensions can be summarized as shown in Figure 8. When the molecular weight ratio was high, the symmetric PS-*r*-PVP was able to assemble at the interface of PS-*b*-PVP, reducing the unfavorable interaction between the PS and PVP segments. The localized PS-*r*-PVP at the PS-*b*-PVP interface caused lateral expansion along the interface, which caused a contraction of the interdomain distance of the blends. With increasing PS-*r*-PVP concentration, the interfacial region was saturated and the excess PS-*r*-PVP was unable to locate at the PS-*b*-PVP interface. Hence, PS-*r*-PVP was expelled from the ordered domains, forming macrophase separation. By contrast, when the highly asymmetric PS-*r*-PVP was mixed with PS-*b*-PVP, PS-*r*-PVP acted as a homopolymer that was sequestered into the preferred domain of PS-*b*-PVP. The confined PS-*b*-PVP expanded the preferred domain and changed the interfacial curvature between PS and PVP microdomains, which induced an order−order transition. Conversely, when the molecular weight ratio was low, the incorporation of PS-*r*-PVP in the PS-*b*-PVP microdomains caused an entropic penalty and macrophase separation at low PS-*r*-PVP concentrations. The present systematic study contributes experimental data to the scarce literature on the phase behavior of block copolymer/random copolymer blends. The knowledge gained in this study can serve as a reference in controlling morphology and domain dimension in the fabrication of polymer blends for various nanotechnological applications.

■ ASSOCIATED CONTENT

Supporting Information

Infrared spectra and ^{1}H NMR of PS-*r*-PVP. This material is available free of charge via the Internet at http://pubs.acs.org.

■ AUTHOR INFORMATION

Corresponding Author

*E-mail: tsunglo@mail.ncku.edu.tw. Phone: +886-6-2757575, ext 62647. Fax: +886-6-2344496.

Notes

The authors declare no competing financial interest.

■ ACKNOWLEDGMENTS

This work was financially supported by National Science Council in Republic of China under Grant No. NSC 99-2628-E-006-001 and NSC 102-2221-E-006-018-MY3.

REFERENCES

(1) Leibler, L. Theory of Microphase Separation in Block Copolymers. *Macromolecules* **1980**, *13*, 1602−1617.

(2) Bates, F. S.; Fredrickson, G. H. Block Copolymer Thermodynamics − Theory and Experiment. *Annu. Rev. Phys. Chem.* **1990**, *41*, 525−557.

(3) Hamley, I. W. *The Physics of Block Copolymers*; Oxford University Press: New York, 1998.

(4) Fasolka, M. J.; Mayes, A. M. Block Copolymer Thin Films: Physics and Applications. *Annu. Rev. Mater. Res.* **2001**, *31*, 323−355.

(5) Hashimoto, T.; Shibayama, M.; Fujimura, M.; Kawai, H. In *Block Copolymers, Science and Technology*; Meier, D. J., Ed.; Harwood Academic: London, 1983.

(6) Cohen, R. E. Block Copolymers as Templates for Functional Materials. *Curr. Opin. Solid State Mater. Sci.* **1999**, *4*, 587−590.

(7) Förster, S.; Antonietti, M. Amphiphilic Block Copolymers in Structure-Controlled Nanomaterial Hybrids. *Adv. Mater.* **1998**, *10*, 195−217.

(8) Xuan, Y.; Peng, J.; Cui, L.; Wang, H.; Li, B.; Han, Y. Morphological Development of Ultrathin Symmetric Diblock Copolymer Film via Solvent Vapor Treatment. *Macromolecules* **2004**, *37*, 7301−7307.

(9) Hashimoto, T.; Tanaka, H.; Hasegawa, H. Ordered Structure in Mixtures of a Block Polymer and Homopolymers. 2. Effects of Molecular-Weights of Homopolymers. *Macromolecules* **1990**, *23*, 4378−4386.

(10) Tanaka, H.; Hasegawa, H.; Hashimoto, T. Ordered Structure in Mixtures of a Block Polymer and Homopolymers. 1. Solubilization of Low-Molecular-Weight Homopolymers. *Macromolecules* **1991**, *24*, 240−251.

(11) Tanaka, H.; Hashimoto, T. Thermal Concentration fluctuations of Block Polymer Homopolymer Mixtures in the Disordered State. 1. Binary-Mixtures of SI/HS. *Macromolecules* **1991**, *24*, 5398−5407.

(12) Winey, K. I.; Thomas, E. L.; Fetters, L. J. Ordered Morphologies in Binary Blends of Diblock Copolymer and Homopolymer and Characterization of their Intermaterial Dividing Surfaces. *J. Chem. Phys.* **1991**, *95*, 9367−9375.

(13) Winey, K. I.; Thomas, E. L.; Fetters, L. J. Isothermal Morphology Diagrams for Binary Blends of Diblock Copolymer and Homopolymer. *Macromolecules* **1992**, *25*, 2645−2650.

(14) Matsen, M. W. Phase-Behavior of Block Copolymer Homopolymer Blends. *Macromolecules* **1995**, *28*, 5765−5773.

(15) Likhtman, A. E.; Semenov, A. N. Theory of Microphase Separation in Block Copolymer/Homopolymer Mixtures. *Macromolecules* **1997**, *30*, 7273−7278.

(16) Hashimoto, T.; Yamasaki, K.; Koizumi, S.; Hasegawa, H. Ordered Structure in Blends of Block Copolymers. 1. Miscibility Criterion for Lamellar Block Copolymers. *Macromolecules* **1993**, *26*, 2895−2904.

(17) Hashimoto, T.; Koizumi, S.; Hasegawa, H. Ordered Structure in Blends of Block Copolymers. 2. Self-Assembly for immiscible Lamellar-Forming Copolymers. *Macromolecules* **1994**, *27*, 1562−1570.

(18) Court, F.; Hashimoto, T. Morphological Studies of Binary Mixtures of Block Copolymers. 1. Cosurfactant Effects and Composition Dependence of Morphology. *Macromolecules* **2001**, *34*, 2536−2545.

(19) Yamaguchi, D.; Hashimoto, T. A Phase Diagram for the Binary Blends of Nearly Symmetric Diblock Copolymers. 1. Parameter Space of Molecular Wight Ratio and Blend Composition. *Macromolecules* **2001**, *34*, 6495−6505.

(20) Court, F.; Hashimoto, T. Morphological Studies of Binary Mixtures of Block Copolymers. 2. Chain Organization of Long and Short Blocks in Lamellar Microdomains and its Effect on Domain Size and Stability. *Macromolecules* **2002**, *35*, 2566−2575.

(21) Court, F.; Yamaguchi, D.; Hashimoto, T. Morphological Studies of Binary Mixtures of Block Copolymers: Temperature Dependence of Cosurfactant Effects. *Macromolecules* **2006**, *39*, 2596−2605.

(22) Kressler, J.; Karasz, F. E.; Kammer, H. W.; Morgenstern, U. Miscibility in Blends of Random Copolymers of Styrene and Acrylontrile with Block Copolymers of Styrene and Methyl-Methacrylate. *Makromol. Chem.* **1990**, *191*, 1623−1631.

(23) Lee, H.-K.; Zin, W.-C. Phase Diagrams for the Blends of a Styrene-Butadiene Diblock Copolymer and a Styrene-Butadiene Random Copolymer: Theory. *Macromolecules* **2000**, *33*, 2894−2900.

(24) Kim, D.-C.; Lee, H.-K.; Sohn, B.-H.; Zin, W.-C. Order−Disorder Transition Temperature Depression of a Diblock Copolymer Induced by the Addition of a Random Copolymer. *Macromolecules* **2001**, *34*, 7767−7772.

(25) Lee, H.-K.; Kim, D.-C.; Yoo, S. I.; Sohn, B.-H.; Zin, W.-C. Phase Diagram for Blends of Styrene-Butadiene Diblock Copolymer and Styrene-Butadiene Random Copolymer. *Macromolecules* **2003**, *36*, 7740−7745.

(26) Kim, D.-C.; Yoo, S. I.; Moon, S.-W.; Zin, W.-C. Effect of Composition of Added Random Copolymer on the Phase Behavior of Block Copolymer. *Polymer* **2005**, *46*, 6595−6604.

(27) Dai, C.-A.; Osuji, C. O.; Jandt, K. D.; Dair, B. J.; Ober, C. K.; Kramer, E. J.; Hui, C.-Y. Effect of the Monomer Ratio on the Strengthening of Polymer Phase Boundaries by Random Copolymers. *Macromolecules* **1997**, *30*, 6727−6736.

(28) Brown, F. E.; Ham, G. E. General Conclusions about Copolymerization of ethylene with Other Monomers by Free Radical Catalysis. *J. Polym. Sci., Part A* **1964**, *A2*, 3623.

(29) Chang, C.-J.; Lee, Y.-H.; Chiang, C.-J.; Lee, Y.-P.; Chien, H.-C.; Shih, W.-P.; Cheng, Y.-Y.; Dai, C.-A.; Chang, C.-H. Strength of Polymer Phase Boundaries with Large Interfacial Width: Effects of Interfacial Profile and Phase Separation Morphology. *J. Polym. Sci., Polym. Phys. Ed.* **2010**, *48*, 1834−1846.

(30) Gersappe, D.; Balazs, A. C. Random Copolymers as Effective Compatibilizing Agents. *Phys. Rev. E* **1995**, *52*, 5061−5064.

(31) Milner, S. T.; Fredrickson, G. H. Interfacial Strengthening with Random Copolymers. *Polym. Mater. Sci. Eng.* **1996**, *75*, 80.

(32) Milner, S. T.; Fredrickson, G. H. Reconsidering Random Copolymers at Interfaces. *Macromolecules* **1995**, *28*, 7953−7956.

(33) Chen, Y.-T.; Lo, C.-T. Self-Assembled Structures in Block Copolymer/Graft Copolymer Blends with Hydrogen Bonding Interaction. *Soft Matter* **2013**, *9*, 1756−1760.

(34) Matsushita, Y.; Torikai, N.; Mogi, Y.; Noda, I.; Han, C. C. Localization of a Homopolymer Dissolved in a Lamellar Structure of a Block-Copolymer Studied by Small-Angle Neutron-Scattering. *Macromolecules* **1993**, *26*, 6346−6349.

(35) Torikai, N.; Takabayashi, N.; Noda, I.; Koizumi, S.; Morii, Y.; Matsushita, Y. Lamellar Domain Spacings of Diblock Copolymer/Homopolymer Blends and Conformations of Block Chains in their Microdomains. *Macromolecules* **1997**, *30*, 5698−5703.

dx.doi.org/10.1021/jp5062607 | *J. Phys. Chem. B* 2014, 118, 12763−12771